Electronic Supplementary Material (ESI) for Faraday Discussions.

Supporting Information

Effect of Liquid Confinement on Regioselectivity in the Hydrosilylation of Alkynes With Cationic Rh (I) *N*-Heterocyclic Carbene Catalysts

Pradeep K. R. Panyam, Michael R. Buchmeiser*

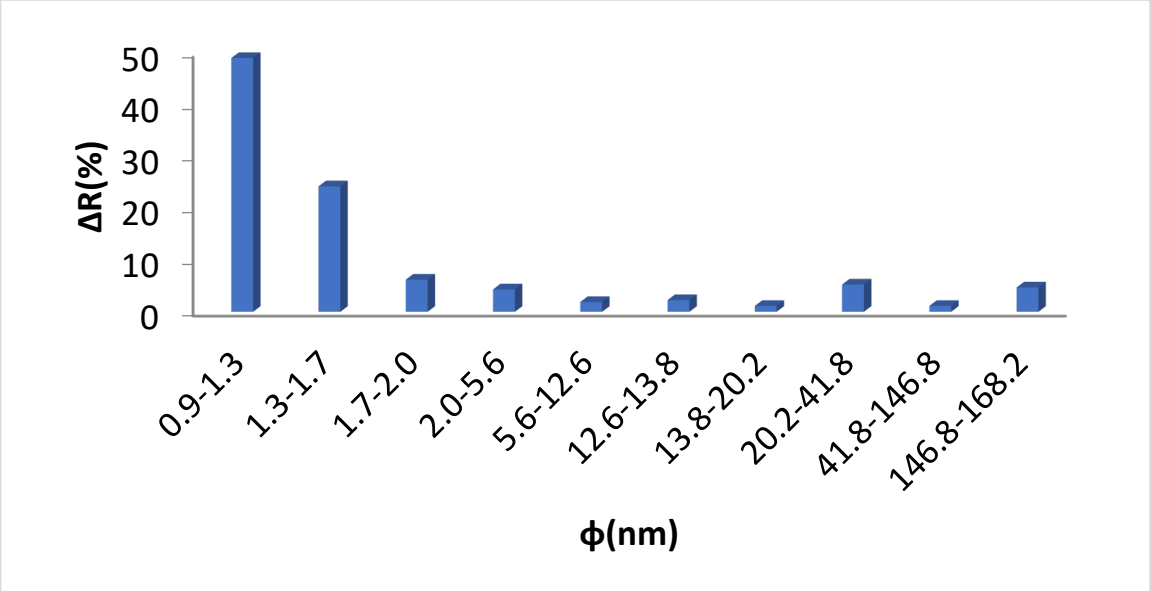

Figure S1. Representative pore size distribution of a ROMP-derived monolith. Relative abundance ΔR (%) of pores with different diameters Φ (nm).

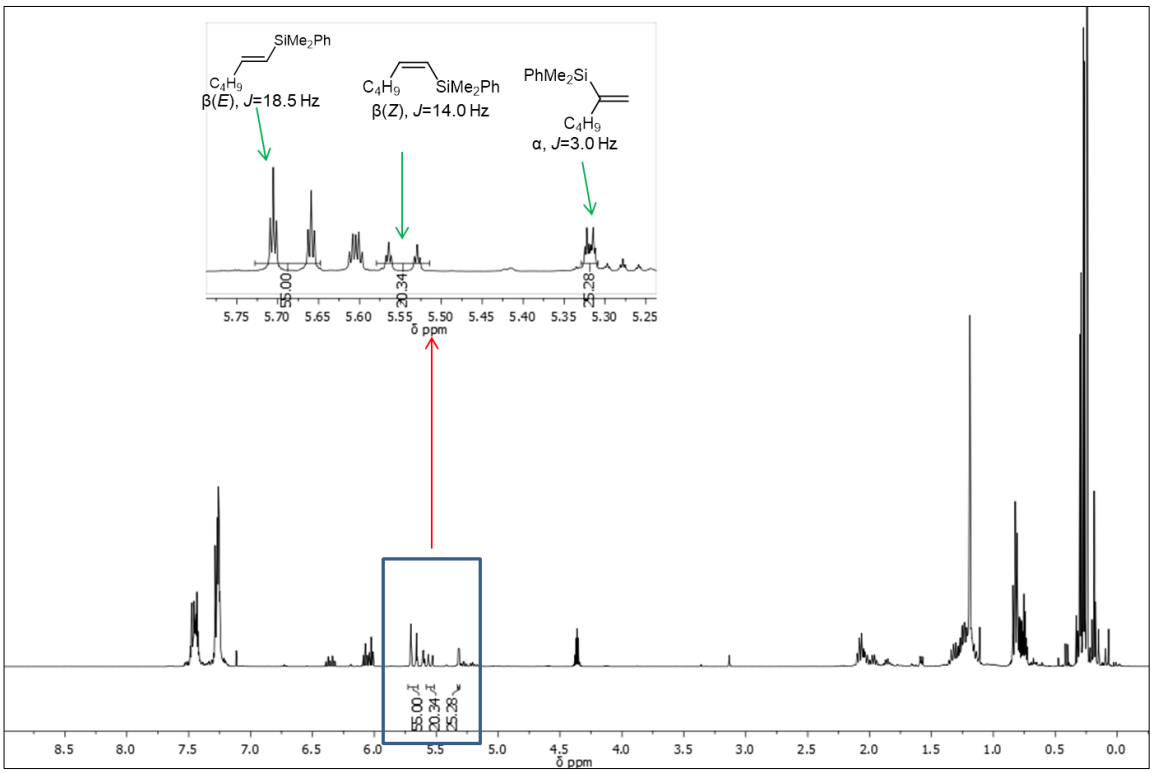

Figure S2. ^{1}H NMR spectrum ($CDCl_3$, 298K) of the hydrosilylation of 1-hexyne with $HSiMe_2Ph$ catalyzed by **Rh@biphasic**.

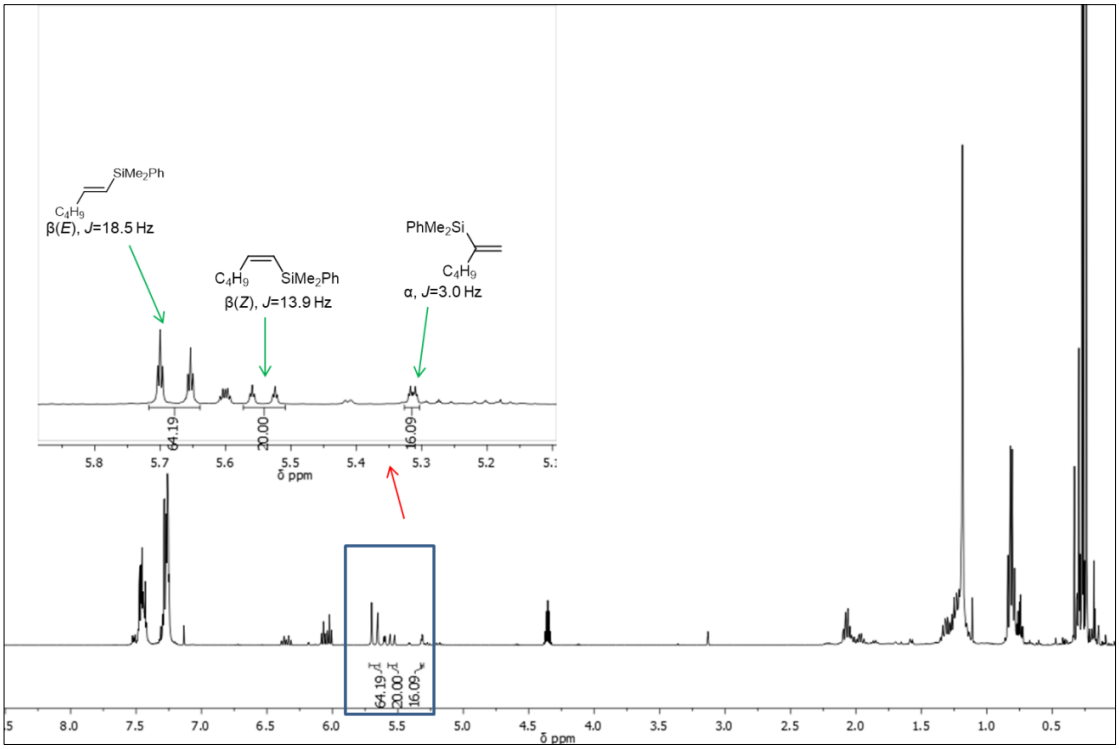

Figure S3. ^{1}H NMR spectrum ($CDCl_3$, 298K) of the hydrosilylation of 1-hexyne with $HSiMe_2Ph$ catalyzed by **Rh@SILPR$_{ROMP-0}$**.

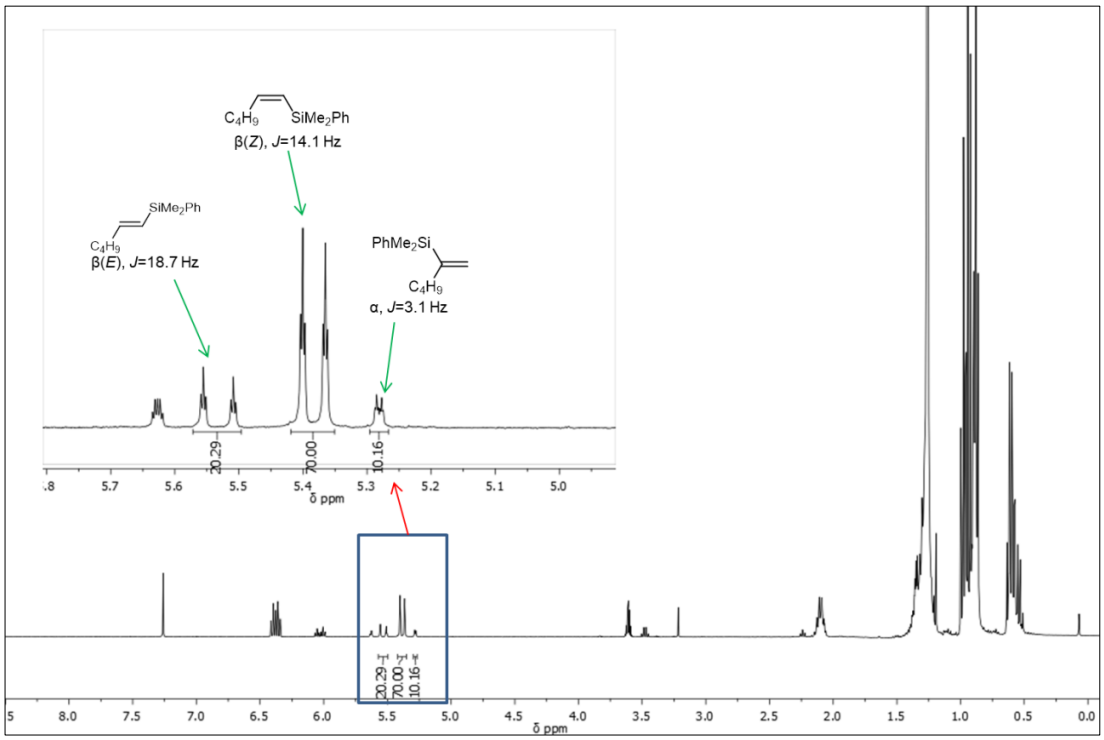

Figure S4. ^{1}H NMR spectrum ($CDCl_3$, 298K) of the hydrosilylation of 1-hexyne with $HSiMe_2Ph$ catalyzed by **Rh@SILP$_{ROMP-10}$**.

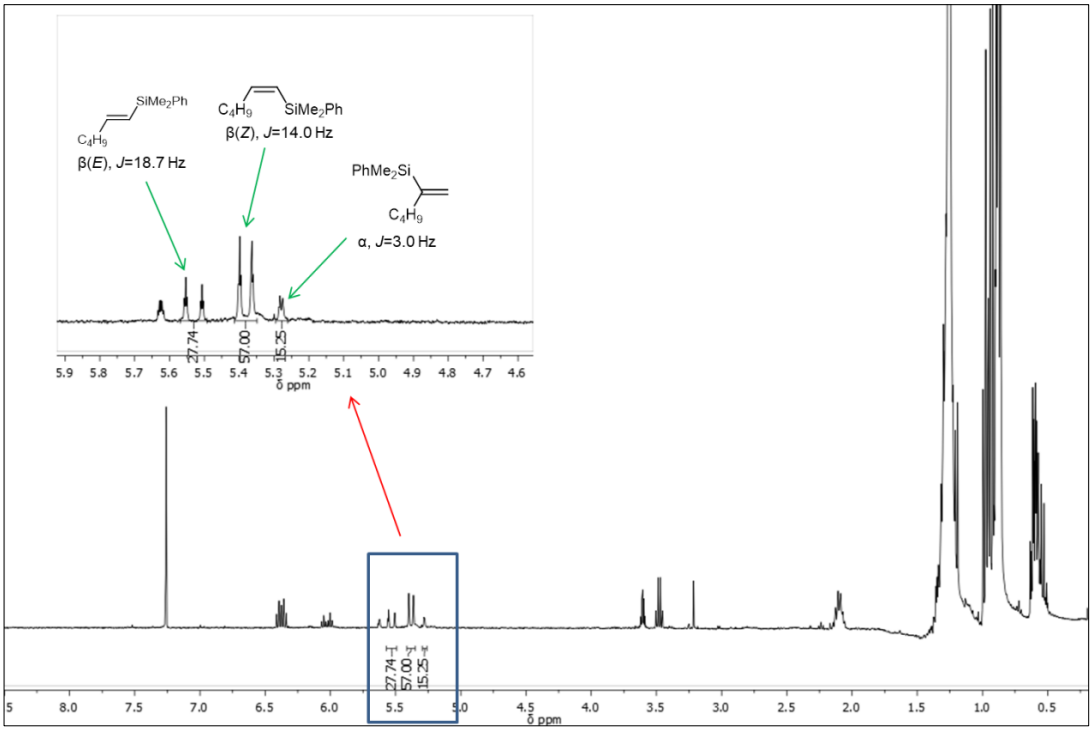

Figure S5. ^{1}H NMR spectrum ($CDCl_3$, 298K) of the hydrosilylation of 1-hexyne with $HSiMe_2Ph$ catalyzed by **Rh@SILP$_{ROMP-25}$**.

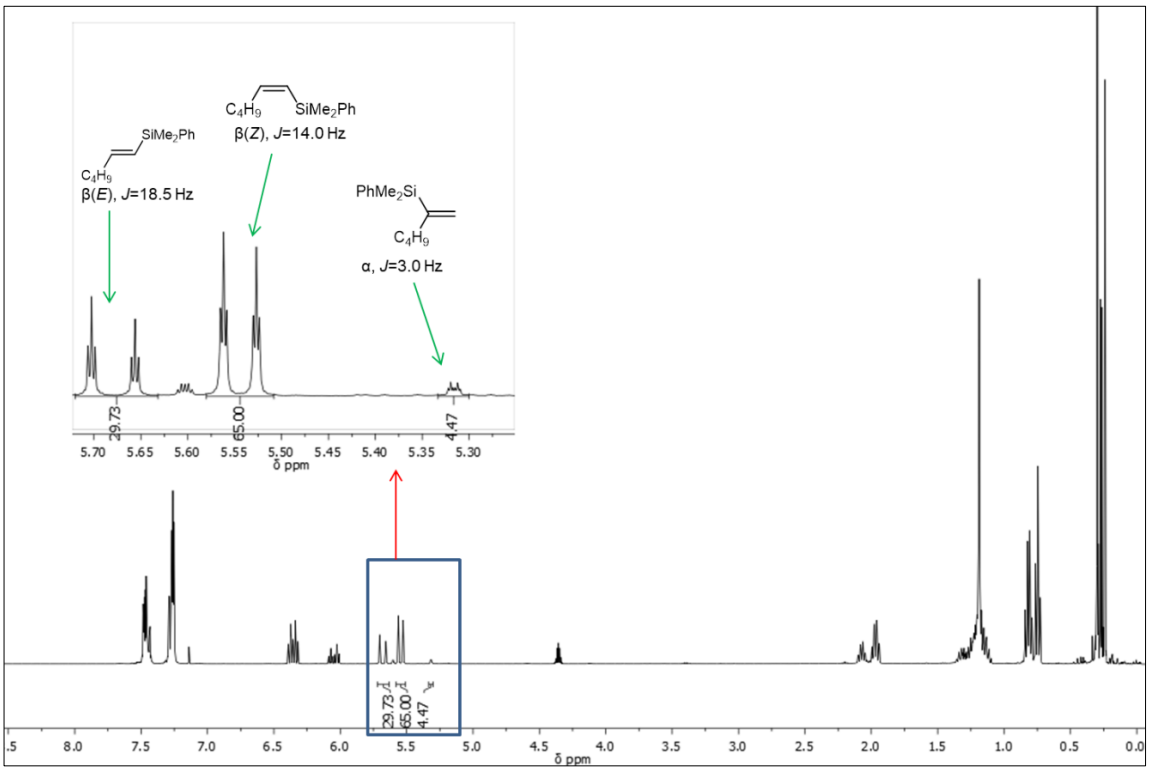

Figure S6. ^{1}H NMR spectrum ($CDCl_3$, 298K) of the hydrosilylation of 1-hexyne with $HSiMe_2Ph$ catalyzed by **Rh@SILP$_{ROMP-50}$**.

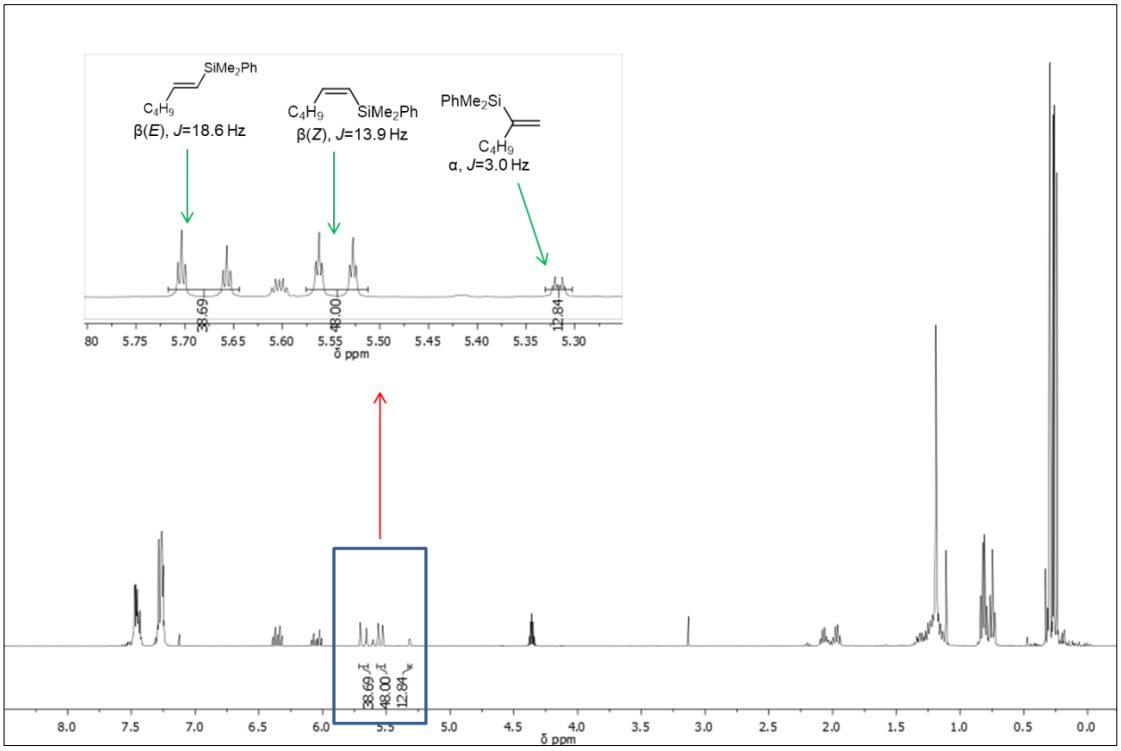

Figure S7. ^{1}H NMR spectrum ($CDCl_3$, 298K) of the hydrosilylation of 1-hexyne with $HSiMe_2Ph$ catalyzed by **Rh@SILP$_{ROMP\text{-}100}$**.

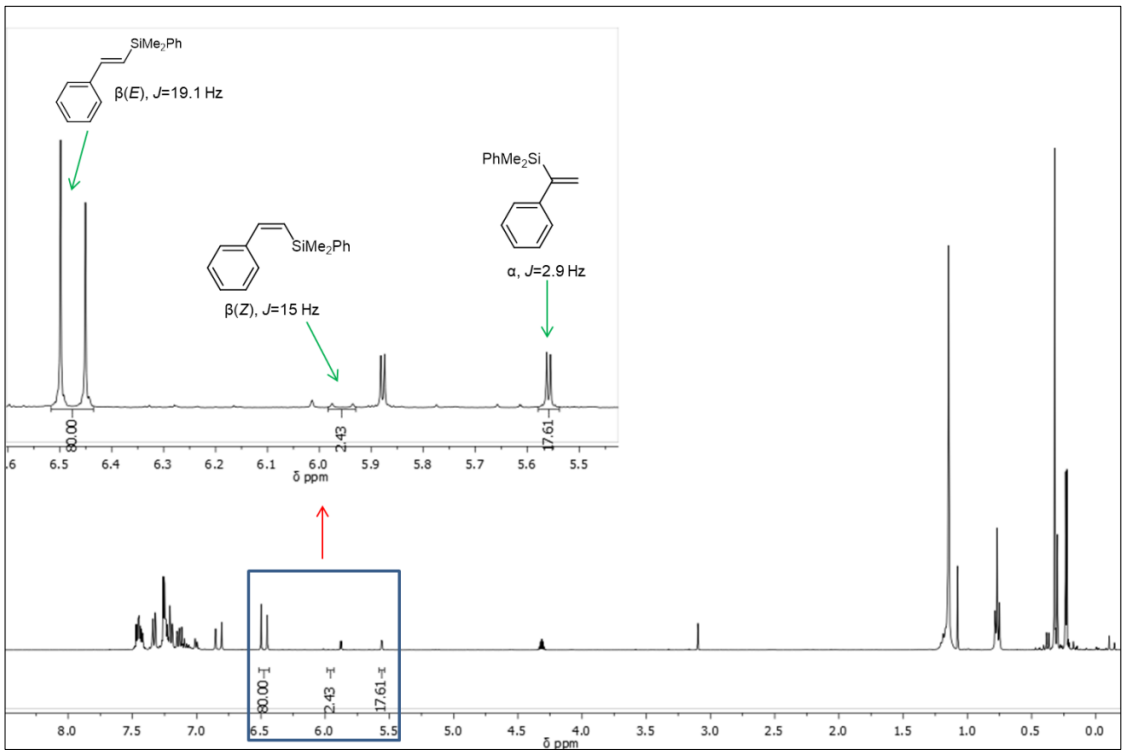

Figure S8. ^{1}H NMR spectrum ($CDCl_3$, 298K) of the hydrosilylation of phenylacetylene with $HSiMe_2Ph$ catalyzed by **Rh@biphasic**.

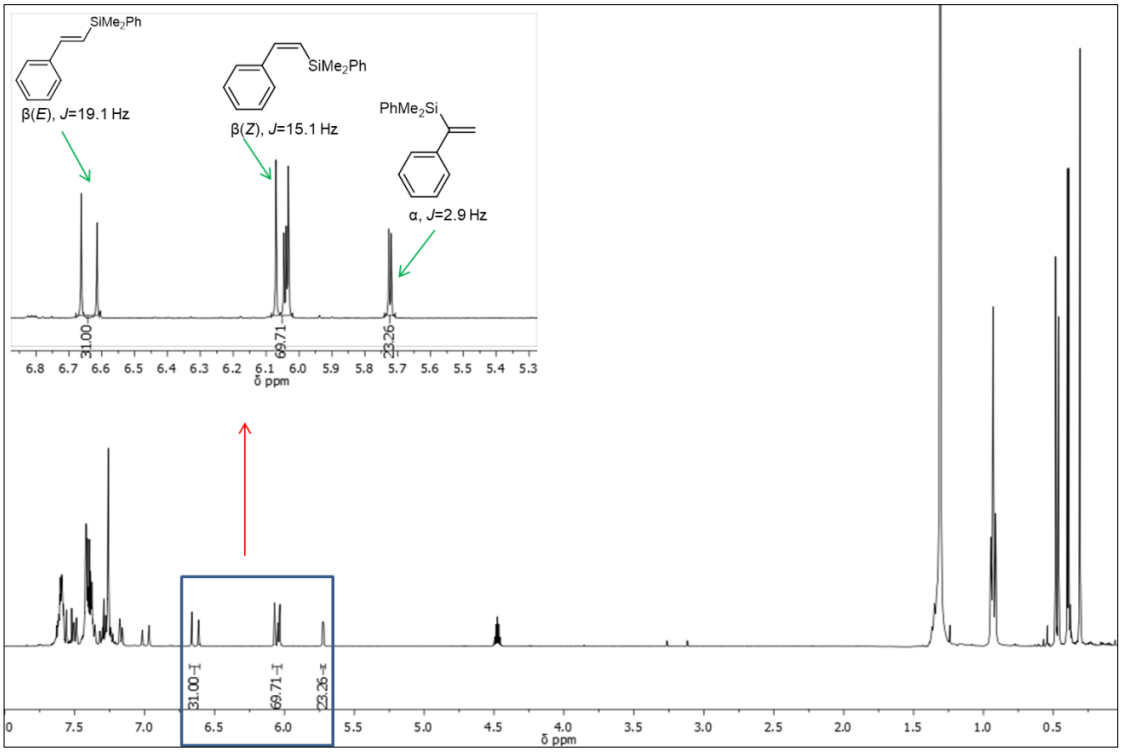

Figure S9. ^{1}H NMR spectrum ($CDCl_3$, 298K) of the hydrosilylation of phenylacetylene with $HSiMe_2Ph$ catalyzed by **Rh@SILP$_{ROMP\text{-}100}$** (exemplary spectrum).

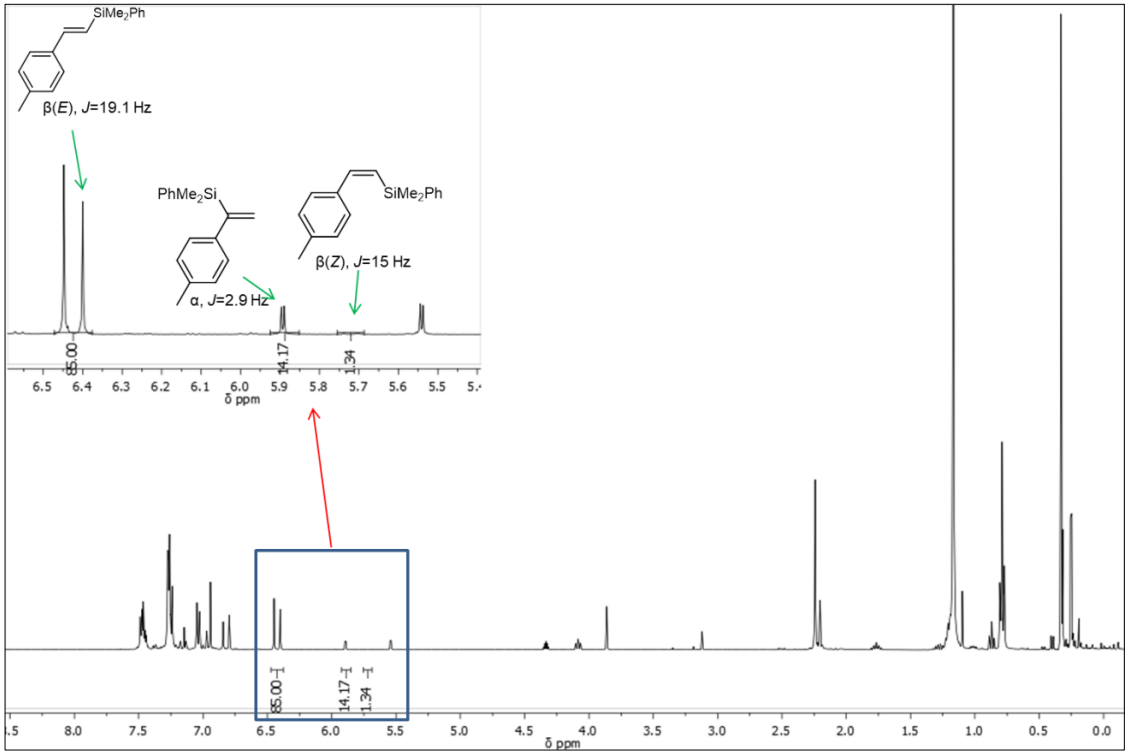

Figure S10. ^{1}H NMR spectrum ($CDCl_3$, 298K) of the hydrosilylation of 4-ethynyltoluene with $HSiMe_2Ph$ catalyzed by **Rh@biphasic**.

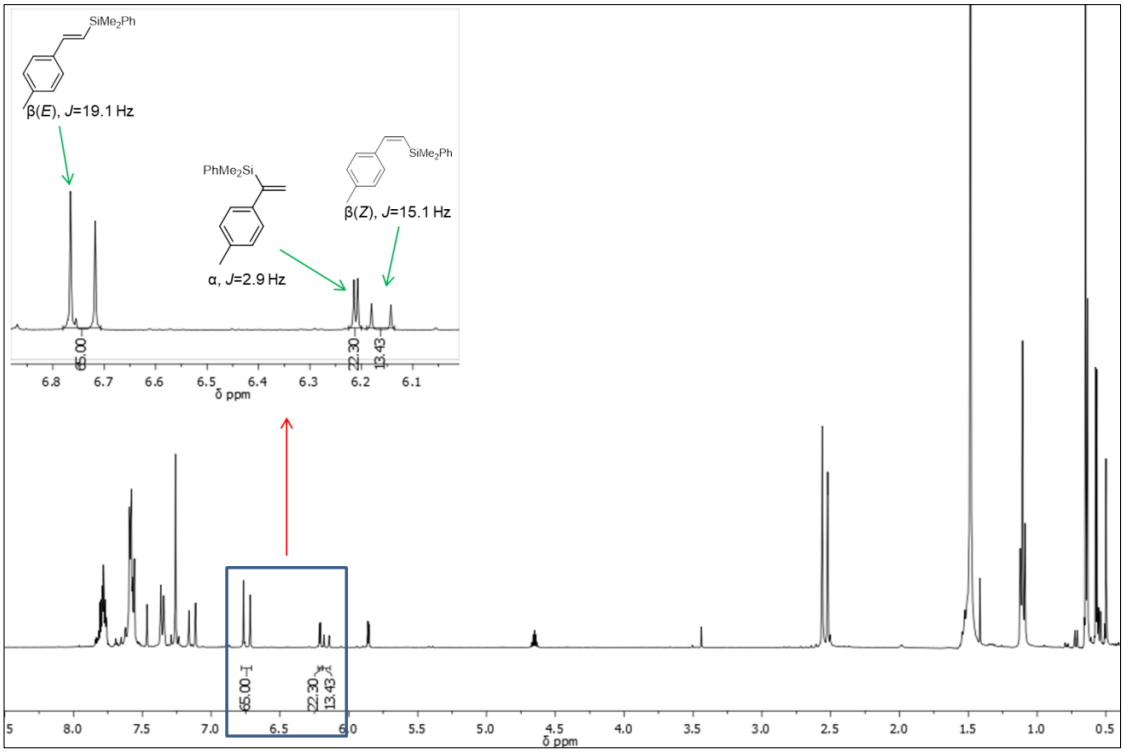

Figure S11. ^{1}H NMR ($CDCl_3$, 298K) of the hydrosilylation of 4-ethynyltoluene with $HSiMe_2Ph$ catalyzed by **Rh@SILP$_{ROMP\text{-}100}$** (exemplary spectrum).

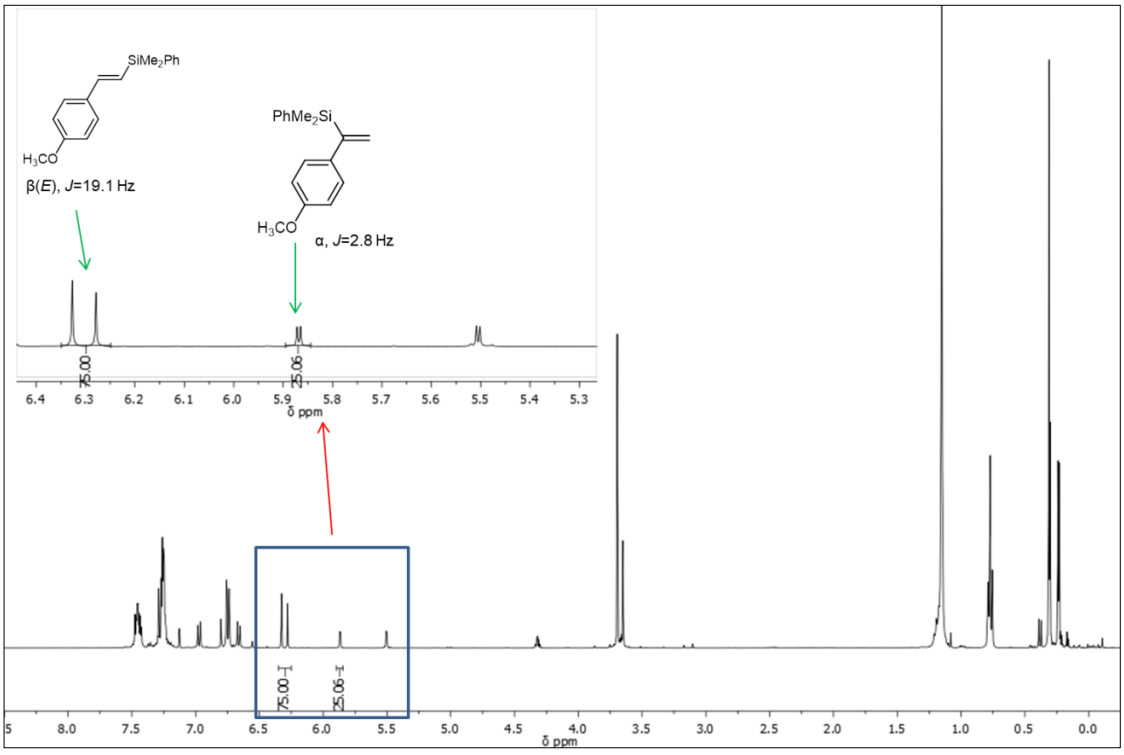

Figure S12. ^{1}H NMR spectrum ($CDCl_3$, 298K) of the hydrosilylation of 4-ethynylanisole with $HSiMe_2Ph$ catalyzed by **Rh@biphasic**.

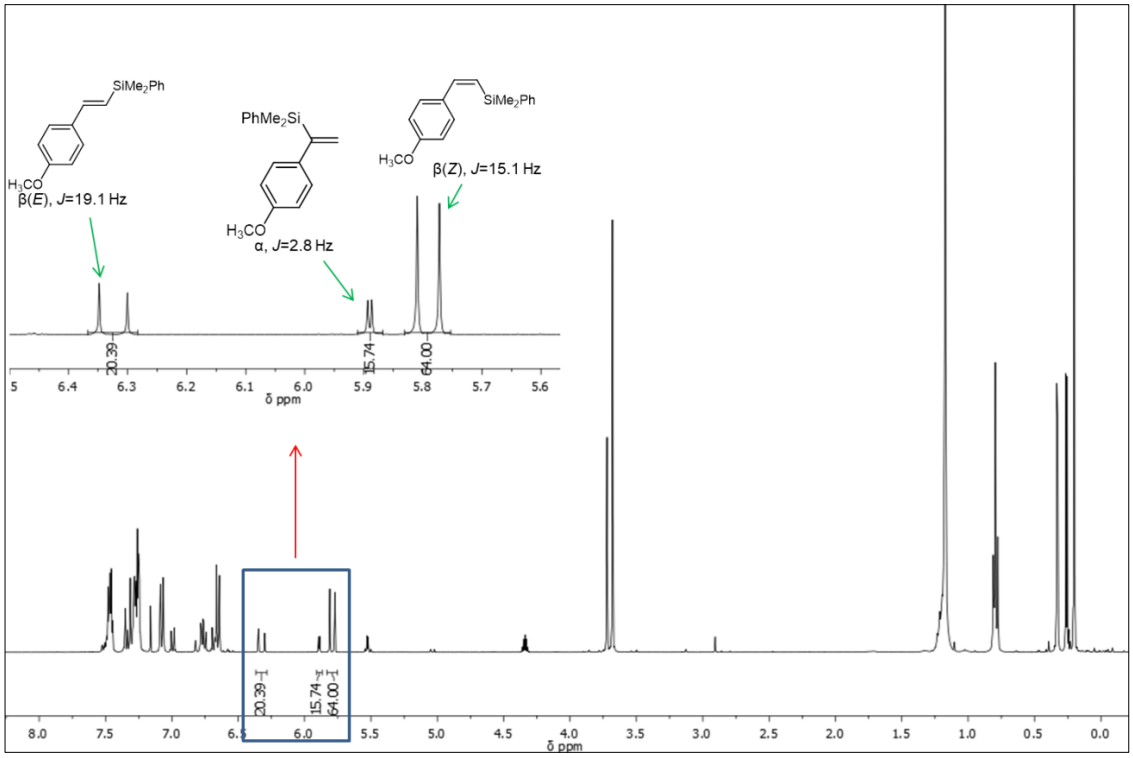

Figure S13. ^{1}H NMR spectrum ($CDCl_3$, 298K) of the hydrosilylation of 4-ethynylanisole with $HSiMe_2Ph$ catalyzed by **Rh@SILP$_{ROMP\text{-}100}$** (exemplary spectrum).

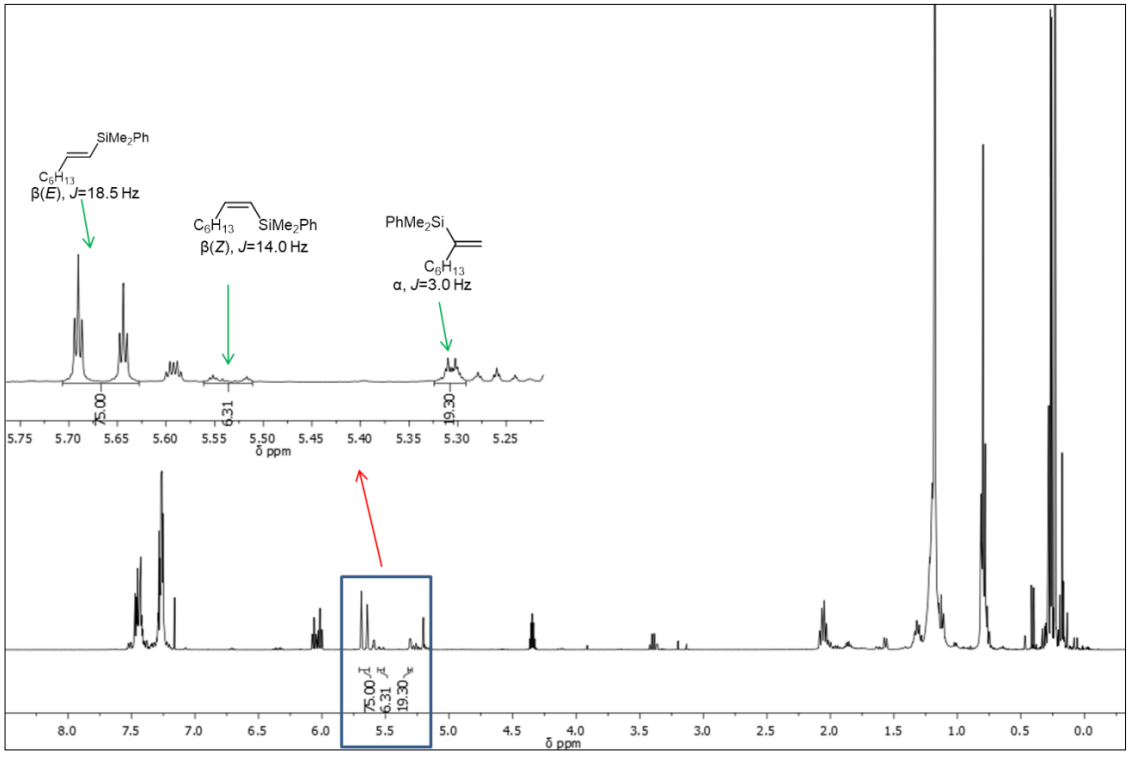

Figure S14. ^{1}H NMR spectrum ($CDCl_3$, 298K) of the hydrosilylation of 1-octyne with $HSiMe_2Ph$ catalyzed by **Rh@biphasic**.

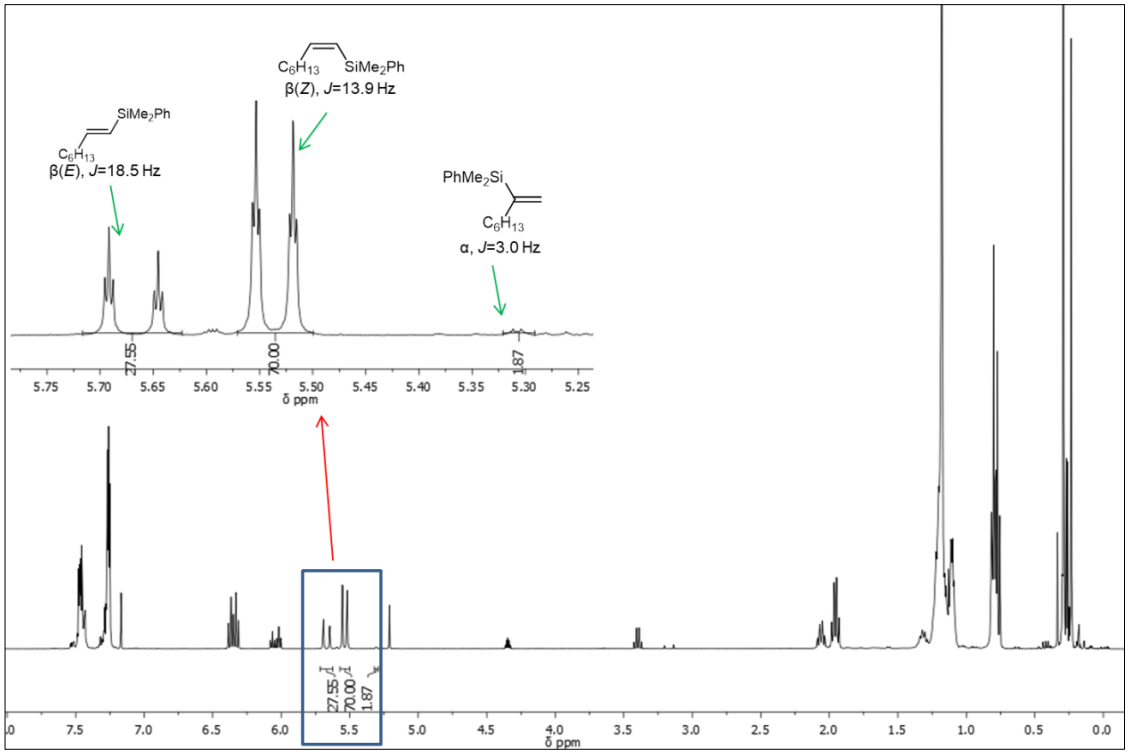

Figure S15. ^{1}H NMR spectrum ($CDCl_3$, 298K) of the hydrosilylation of 1-octyne with $HSiMe_2Ph$ catalyzed by **Rh@SILP$_{ROMP\text{-}100}$** (exemplary spectrum).

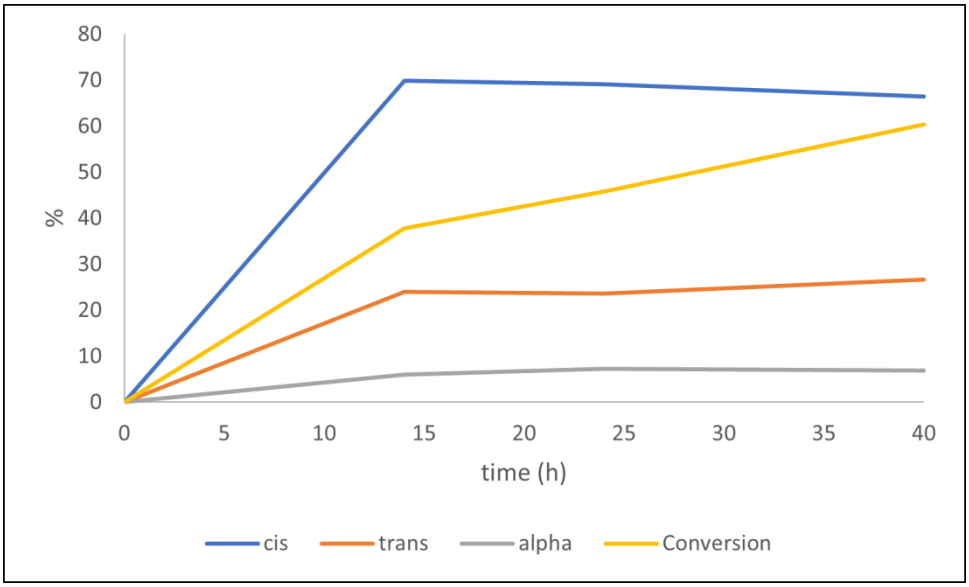

Figure S16. Hydrosilylation of 1-hexyne under continuous flow (0.2 mL/min, **Rh@SILP$_{ROMP\text{-}10}$**).

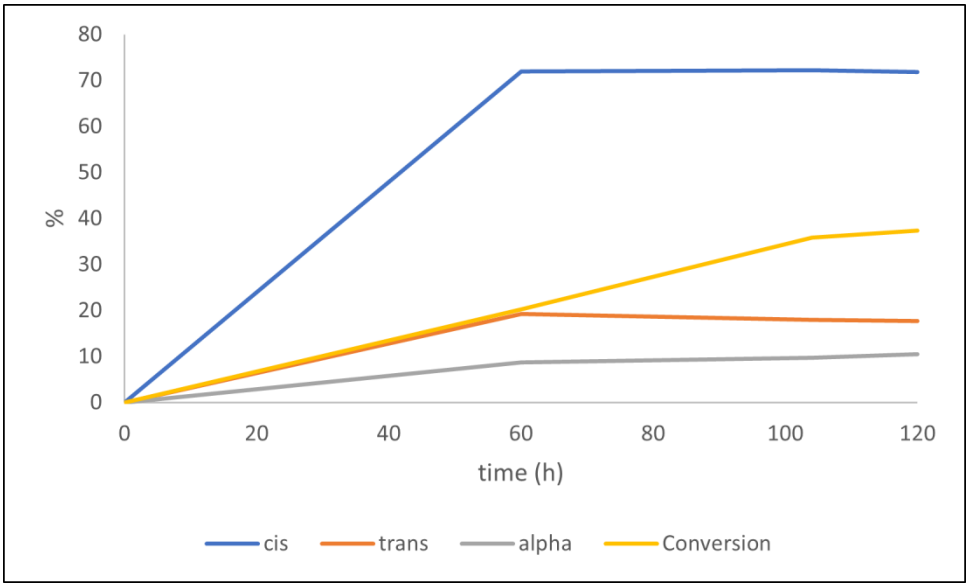

Figure S17. Hydrosilylation of 4-ethynylanisole under continuous flow (0.2 mL/min, **Rh@SILP$_{ROMP-10}$**).

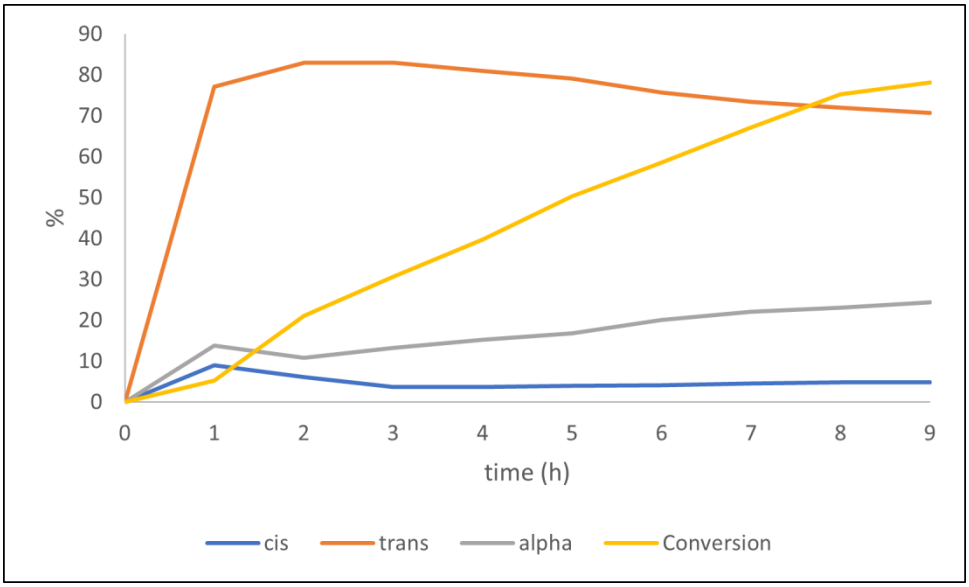

Figure S18. Hydrosilylation of 4-ethynylanisole under biphasic conditions.

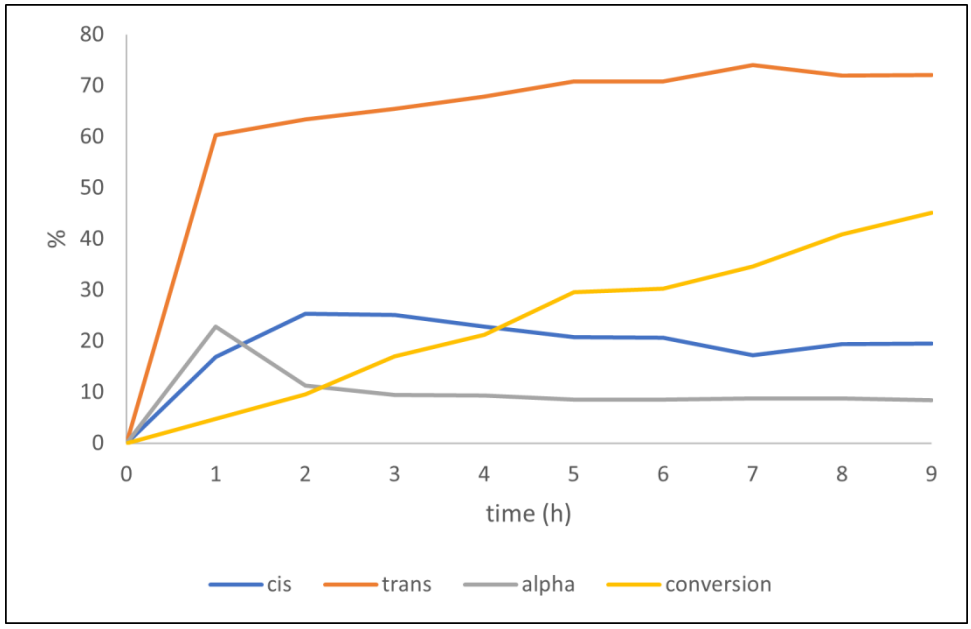

Figure S19. Hydrosilylation of 1-hexyne under biphasic conditions.

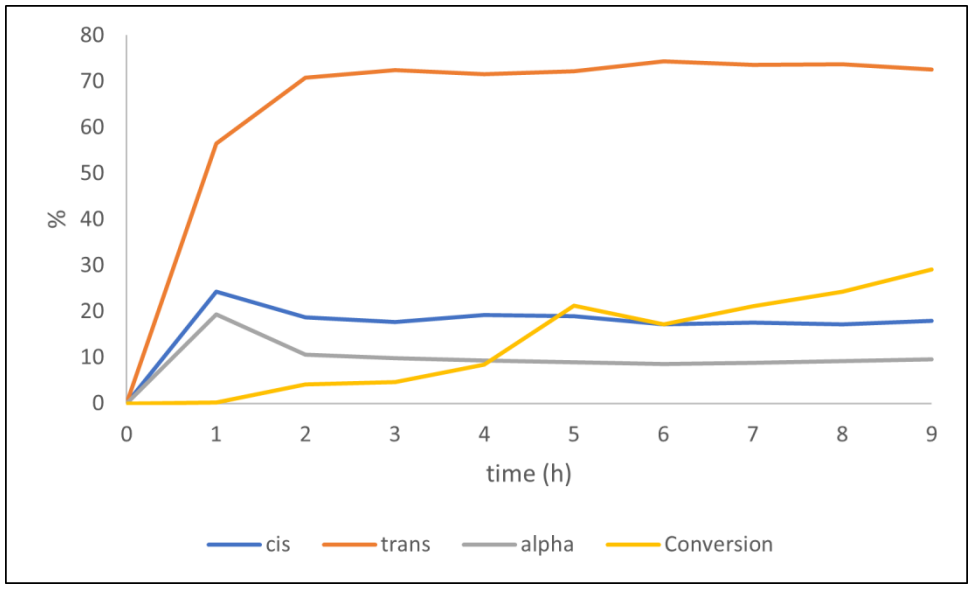

Figure S20. Hydrosilylation of 1-octyne under biphasic conditions.

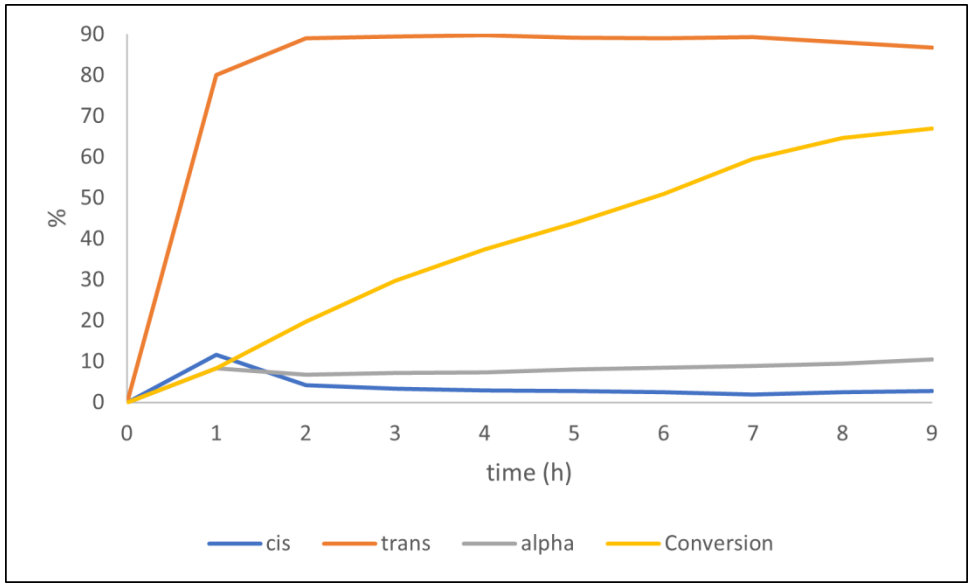

Figure S21. Hydrosilylation of 4-ethynyltoluene under biphasic conditions.

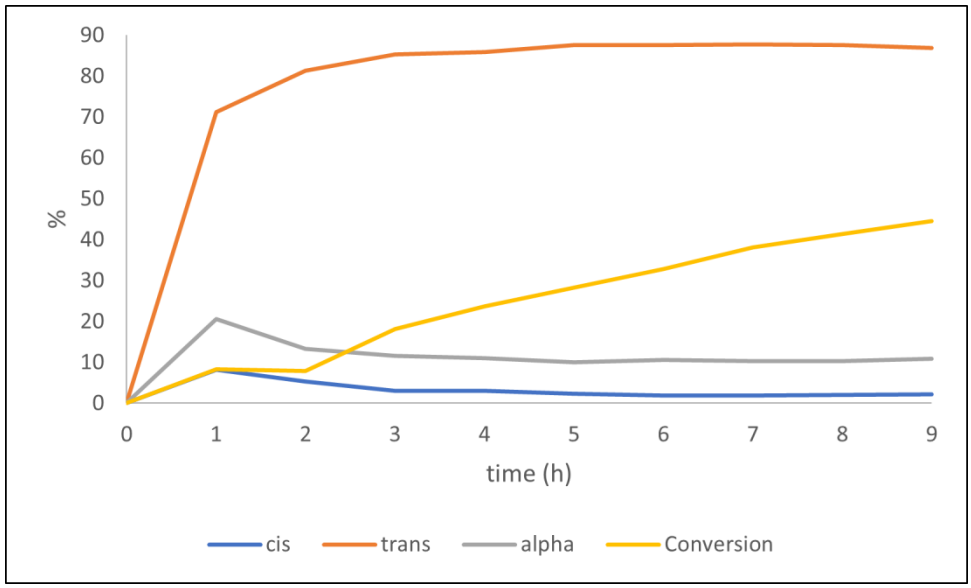

Figure S22. Hydrosilylation of phenylacetylene with $HSiMe_2Ph$ under biphasic conditions.